Transworld Research Network
37/661 (2), Fort P.O., Trivandrum-695 023, Kerala, India

Electromagnetic, Magnetostatic, and Exchange-Interaction Vortices in Confined Magnetic Structures, 2008: 159-175 ISBN: 978-81-7895-373-1 Editor: E.O. Kamenetskii

8 Interaction of a magnetic vortex with non-homogeneous magnetic field of MFM probe

V.L.Mironov and A.A.Fraerman
Institute for physics of microstructures RAS, 603950, Nizhniy Novgorod GSP-105, Russia

Abstract

We investigated both theoretically and experimentally interaction of a magnetic vortex in ferromagnetic nanoparticles with non-homogeneous magnetic field induced by the probe of magnetic force microscope (MFM).

Magnetic force microscopy methods were applied to investigate the peculiarities of magnetic vortex states in elliptical Co nanodisks. Reversible transitions between the uniform and vortex states under non-homogeneous magnetic field of MFM probe were observed. Possibility to control the chirality of a magnetic vortex in these particles by MFM probe manipulation was shown.

The simple model of rigid magnetic vortex is used to describe the probe-vortex interaction. Modeling of

Correspondence/Reprint request: Dr. V.L.Mironov, Institute for physics of microstructures RAS, 603950, Nizhniy Novgorod GSP-105, Russia. E-mail: mironov@ipm.sci-nnov.ru

magnetization redistribution in ferromagnetic nanoparticles under magnetic field induced by MFM probe performed on the base of Landay-Lifshitz-Gilbert equation for magnetization confirms the predicted effects.

The critical transitions between vortex and radial magnetization distributions were predicted. It is shown that the magnetization direction of the core of the vortex can be changed in the MFM probe field without changing of the shell vorticity.

The possible chiral symmetry violation of vortex state in Co nanoparticles was also investigated experimentally.

1. Introduction

In this paper we will consider the potentialities to manipulate by vortex magnetization in ferromagnetic nanodisks by means of non-homogeneous external magnetic field. The non-homogeneous magnetic field can be induced by neighboring ferromagnetic particles [1, 2], Meijssner shielding current in hybrid system ferromagnetic particle / superconductor [3] or by the probe of magnetic force microscope (MFM) [4]. We will focus our attention on the last case due to its comparative simplicity for experimental realization.

In sufficiently thin ferromagnetic disks distribution of magnetization depends only on coordinates in plane of the particle and is described by vector $\vec{M} = \vec{M}(\vec{\rho})$, where $\vec{\rho}$ is the in plane radius vector. Except magneto-crystalline anisotropy and in plane external magnetic field the non-homogeneous distribution of magnetization in the circle disk can be represented in the following form [5]

$$M_x = Sin\,\theta(\rho)\,Cos(\chi + \varphi_0),$$
$$M_y = Sin\,\theta(\rho)\,Sin(\chi + \varphi_0),$$
$$M_z = Cos\,\theta(\rho). \qquad (1)$$

Here ρ is modulus of radius vector $\vec{\rho}$, θ and χ are polar and azimuth angles respectively, φ_0 is arbitrary phase shift. Under well-known conditions [6] the magnetic vortex state (VS) is the ground state of ferromagnetic particle. The topology of this state is determined by phase shift φ_0 and direction of magnetization in the core $\theta_0 = \theta\,(\rho = 0)$. There are four possible combinations of $\varphi_0 = \pm\,\pi / 2$ and $\theta_0 = 0, \pi$, which correspond to the magnetic vortexes with different chirality and core direction. Note that vortex state is fourfold degenerated, i.e. energies of all possible vortex configurations (φ_0, θ_0) are equal. In circle ferromagnetic disks the core orientation can be determined by magnetic force microscopy [7] and vorticity direction can be investigated by electron microscopy methods [8, 9]. In elliptical disks we have additional possibility for observation of vortex chirality by MFM. Indeed in elliptical vortex the effective magnetic charge distribution (proportional to $div\vec{M}(\vec{\rho})$) has a quadrupol moment and the elliptical vorticity becomes apparent in the symmetry of MFM image [10]. External uniform magnetic field in plane of the particle reduces symmetry of the problem. Left and right hand vortexes are removed in opposite directions perpendicular to the external field. At the same time the degeneration of vortex state for perfect elliptical disk in uniform external field is conserved. So, the control of vorticity direction in perfect ferromagnetic disk using uniform magnetic field is impossible. On the other hand, the simulation performed in [9]

shows that even a very small violation of particle shape symmetry leads to the vortex nucleation with preferable chirality. It has been shown experimentally [11] that it is possible to control effectively the vorticity sign if the field of preliminary magnetization has a component in the plane of an asymmetric ferromagnetic disk.

The paper has the following structure. In section 2 we describe briefly our methods for fabrication and investigation of ferromagnetic nanoparticles. In section 3, we consider the peculiarities of probe-vortex interaction and show the possibility to control vorticity direction in elliptical particles using non-homogeneous magnetic field induced by MFM tip. In section 4 we consider possibility for creation hedgehog-like states ($\varphi_0 = 0, \pi$) in ferromagnetic particles under the action of non-homogeneous magnetic field. In section 5 we discuss possibility for taking down degeneration of vortex states due to coupling between phase φ_0 and core polarization θ_0 .

2. Experimental techniques and methods

The rectangular lattices of elliptical Co disks with different sizes of elements and different periods were fabricated by the e-beam lithography in a JEM-2000EX electron microscope and subsequent Ar^+ ion etching of thin Co films [2]. The characteristic lateral sizes of particles were varied in 300 ÷ 900 nm (aspect ratio in the range of 1.3 - 1.7), heights of particles were 10 ÷ 30 nm.

The distribution of remanent magnetization and processes of local remagnetization in Co nanodisks were studied using multimode scanning probe microscopes "Solver-PRO" and "Solver-HV". The MFM probes had a Co coating with the thickness in the range of 30-60 nm. The tips were magnetized before measurements along symmetry axes (Z) in 10^4 Oe external magnetic field. MFM measurements were performed in the non contact constant height mode. The phase shift of cantilever oscillations under the gradient of sample magnetic field was registered as the MFM contrast. Scanning height parameters for MFM imaging and for remagnetization procedure were optimized experimentally.

The computer simulations of interaction between magnetization in ferromagnetic nanodisks and MFM probe magnetic field were performed by means of special software (the program was developed in the laboratory of mathematical methods and numerical simulation at the Institute for physics of microstructures RAS). Modeling was curried out on the base of Landay-Lifshitz-Gilbert (LLG) equation for magnetization $\vec{M}(\vec{\rho},t)$ in the MFM probe field:

$$\frac{\partial \vec{M}}{\partial t} = -\frac{\gamma}{1+\alpha^2}[\vec{M}\vec{H}_{eff}] - \frac{\alpha\gamma}{(1+\alpha^2)M_s}[\vec{M}[\vec{M}\vec{H}_{eff}]], \tag{2}$$

where γ is the gyromagnetic ratio, α is the dimensionless damping parameter and M_s is magnetic moment in saturation. The effective field $\vec{H}_{eff} = -\frac{\delta E}{\delta \vec{M}}$ is a variation derivative of the energy function. The total energy of the particle is defined by

$$E = E_{ex} + E_m + E_h . \tag{3}$$

The first term E_{ex} is the energy of the exchange interaction, the second term E_m is the demagnetization energy of the particles. Expressions for these terms have conventional

form (see, for example, [12]). The last term E_h is the energy of the interaction between the magnetization and the non-uniform external magnetic field $\vec{H}$. In calculations the MFM probe was approximated as a uniformly magnetized sphere with effective magnetic moment $m_p = M_{sp}V_p$ (M_{sp} is the remanent magnetization of probe capping material, V_p is the effective volume of the interactive part of magnetic layer of MFM tip). In calculation we used typical values M_{sp} = 1400 G (for Co coated tips), V_p = 0.25÷1.25 10^{-16} cm^3 and scanning heights in the range from 15 nm to 50 nm.

To avoid a three-dimensional grid problem, which needs large computer resources, we assumed that magnetization of a disk does not depend on the z coordinate along the cylindrical axis. Then we integrated the relations for the energy over z and obtained the energy as a function of the magnetization, which is a function of only two space variables. The effective field $\vec{H}_{eff}$ does not depend on z either, so we have a three-dimensional problem reduced to the two-dimensional one. All calculations were carried out for parameters of cobalt J = 10^{-6} erg/cm, M_s = 1400 G. We omitted magnetic anisotropy term in (3), assuming polycrystalline structure of the particles.

3. MFM probe induced changing vortex chirality in elliptical Co nanodisks

MFM probe effects on the magnetic states of ferromagnetic nanoparticles of different shape were discussed earlier in [13-15], but the efforts were basically concentrated on study of the magnetization reversal of uniform states. Here we discuss MFM probe induced transitions between the vortex state (VS) and the uniform state (US) in elliptical Co nanodisks, which demonstrate a possibility to control the magnetic vortex chirality. A method to create VS with a definite orientation of the magnetic vortex (clockwise VS^+ or counterclockwise VS^-) under magnetizing in a homogeneous external field was suggested in [11]. To enhance the probability of vortex nucleation with selected vorticity, authors used the factor of asymmetric particle shape. Here we consider a different approach based on a possibility to control the chirality in symmetric elliptic particles by means of two stage $VS^{+(-)} \Rightarrow US \Rightarrow VS^{-(+)}$ processes in the non-homogeneous magnetic field of the MFM probe [16-18].

As it is well known, both US and VS can be realized in ferromagnetic small particles depending on a ratio of lateral sizes and height [19]. In our experiments we used arrays of elliptical Co disks with lateral sizes 400 × 600 nm. Micromagnetic modeling [20] and MFM measurements show that for these particles there is a characteristic height h^* about 25 nm, which separates the regions of US and VS stability. When the height of particle $h > h^*$, US is getting unstable and VS is realized in the particles [21]. For remagnetization experiments 400 × 600 × 27 nm (height slightly more than h^*) particles array were fabricated. The MFM image of Co particles array (Fig. 1) indicates that the remanent magnetic state of the particles corresponds to VS with different chirality.

Indeed symmetry of MFM images for elliptical vortexes is unambiguously defined by vortex chirality. The magnetization distribution and corresponding MFM contrast calculated for VS^+ and VS^- are presented in Fig. 2(a-d). The typical black-white poles symmetry of the MFM images for elliptical vortex corresponds to quadrupole magnetic moment of magnetization distribution [17, 22].

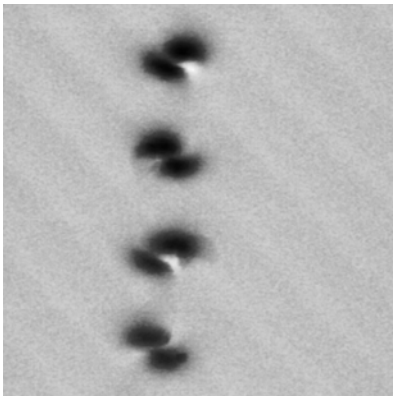

Figure 1. Constant height mode MFM image of the Co particles array. Frame size is 4×4 μm.

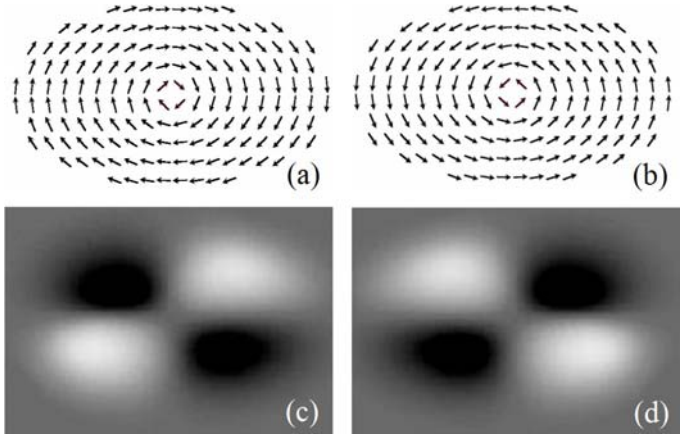

Figure 2. The magnetization distribution and corresponding calculated MFM contrast for clockwise (VS^+) and counterclockwise (VS^-) elliptical vortexes.
(a) is magnetization distribution in VS^+, (b) is magnetization distribution in VS^-,
(c) is calculated MFM image of VS^+, (d) is calculated MFM image of VS^-.

We performed some experiments directed on MFM tip induced changing of VS chirality by special probe manipulations. The main idea was to use magnetic field of MFM probe for realization of VS^+ (or VS^-) $\Rightarrow$ US transition between close energy states for uniform distribution preparation and subsequent US $\Rightarrow$ VS^- (or VS^+) transition by tip induced asymmetric magnetic disturbance of US state to create VS with definite chirality. The results of experiments which illustrated chirality switching by the $VS^+ \Rightarrow US \Rightarrow VS^-$ process are presented in Fig. 3(a-c).

The MFM image of initial state (Fig. 3(a)) was obtained in constant height mode with scanning height (h_s) about 50 nm. As it is clearly seen the initial state of the central particle (indicated by dash line in Fig. 3(a)) corresponds to the clockwise orientation of

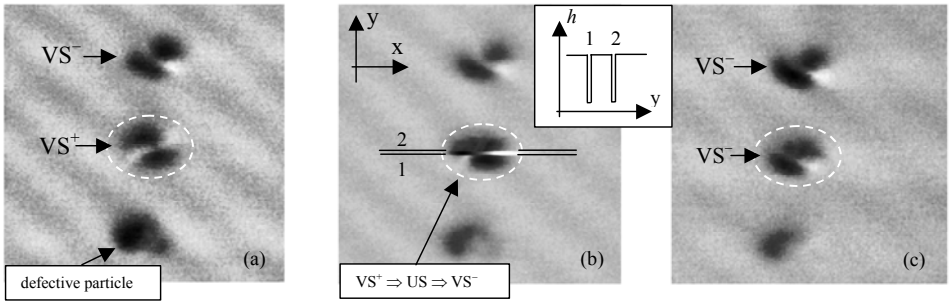

Figure 3. Changing of vortex chirality within a Co particle (central particle indicated by dash line). (a) is the constant height MFM image of the initial state with VS^+ in the central particle. (b) is the MFM image obtained by scanning with variable height. (c) is the final VS^- state in the central particle. Defective particle allows controlling probe position. Frame sizes are 3×3 μm. Insert on Fig. 3(b) shows the probe trajectory $h_s=f(y)$ during manipulation.

vortex (compare with Fig 2(b)). The next image (Fig. 3(b)) was obtained in the following way. At the first stage, scanning was performed in the constant height mode with distance between probe and particles of about 50 nm. When the probe passed over the central particle, the scanning height was reduced to $h_s = 15$ nm in the scan line indicated by number 1 (Fig. 3(b)) whereupon the probe was lifted on 50 nm height again (see insert in Fig. 3(b)). The $VS^+ \Rightarrow$ US transition was registered as the sharp appearance of dipolar MFM contrast. Afterwards, when the probe reached the line indicated by number 2, scanning height was reduced to 15 nm again and US $\Rightarrow VS^-$ transition was observed. At last the constant height MFM image of final state with the counterclockwise vortex orientation in central particle is presented in Fig. 3(c).

We performed computer micromagnetic simulations to describe the remagnetization processes, which were observed under MFM probe manipulations.

The vortex state VS^+ was the initial state in calculations. When the probe moves along the central part of a particle, the vortex shifts to the edge of particle (Fig. 4 (a,b)). The magnetostatic probe - vortex interaction was considered in [23]. The shifted vortex is annihilated at the edge of particle (Fig. 4 (b,c)), so a uniform magnetization distribution is appeared in the area behind the probe (Fig. 4(c,d)). This effect is observed apparently on the line 1 (Fig. 3(b)) as sharp dipolar contrast formation.

The symmetry of US distribution can be destroyed by scanning near the particle edge. Formation of VS in this case is defined by symmetry of the probe magnetic field and probe location near the particle. The US $\Rightarrow VS^-$ process is illustrated in Fig. 5(a-d). At the first stage, when the probe approaches the particle (Fig. 5(a)), chirality of magnetization distribution with direction defined by the MFM probe field is appeared. Indeed, estimation on the base of the Landau-Lifshitz-Gilbert equation shows that the volume averaged z component of chirality for the initial stage is described by the following expression

$$\left\langle \frac{d}{dt}\left(rot\ \vec{M}_{\approx}\right)_z \right\rangle = \alpha \left\langle \frac{\partial H_x}{\partial y} \right\rangle, \qquad (4)$$

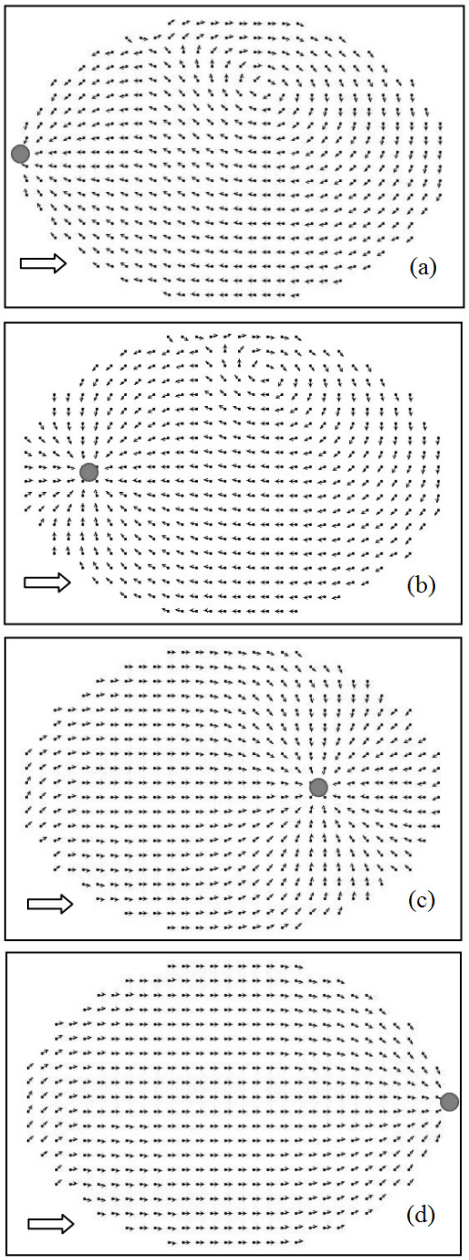

Figure 4. The transition $VS^{+} \Rightarrow US$ under MFM probe movement. (a) is the initial vortex state when probe placed at the left edge of disk. (b) is for shifted vortex just before annihilation. (c) is the distribution after annihilation. (d) is probe induced uniform state. Probe position is indicated by black circle. Scanning direction is shown by white arrow.

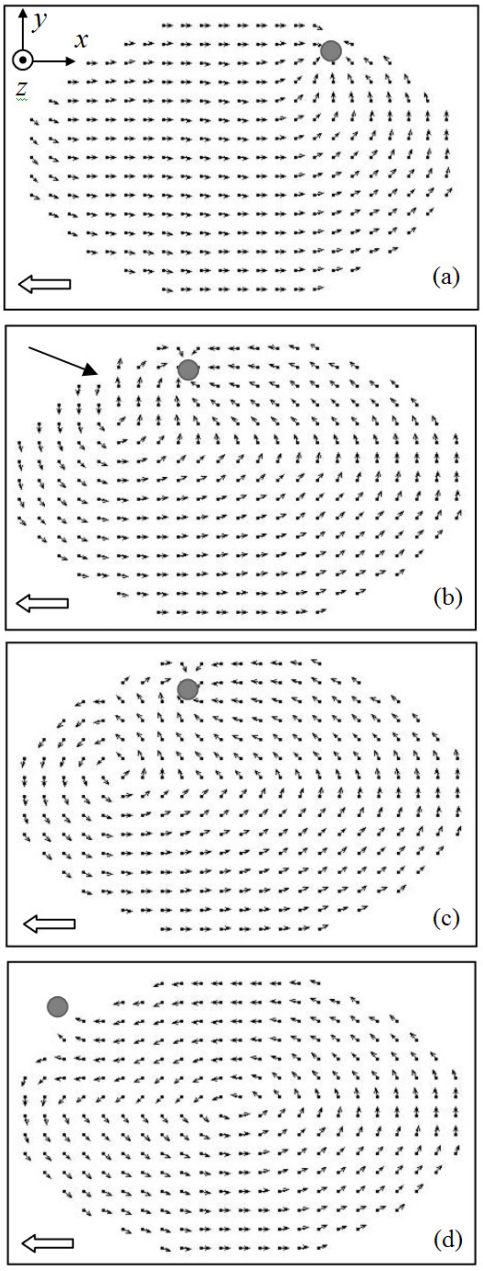

Figure 5. The transition US $\Rightarrow$ VS^{-} under MFM probe movement. (a) is the initial disturbed uniform state when probe placed at the right upper edge of disk. (b) is the fold (indicated by black arrow) where vortex is nucleated. (c) is the vortex appearance. (d) is the final VS^{-} state. Probe position is indicated by black circle and scanning direction by white arrow.

where $\vec{M}_{\sim}$ is the perturbation of magnetization distribution relative to US, α is the damping constant, volume averaging is indicated as < >. As clearly seen, the averaged *z* component of chirality for the initial stage is determined by non-homogeneity of the *x* component of the MFM probe field. From this point of view, the situation represented in Fig. 5(a) corresponds to the vortex nucleation with the counterclockwise orientation. At the next move of the probe a characteristic fold of magnetization is formed near the particle boundary (indicated by black arrow in Fig. 5(b)). The magnetic vortex is nucleated in this fold as shown in Fig. 5(c). After nucleation, the vortex shifts quickly to the center of particle while the probe goes out. The similar US $\Rightarrow$ VS^{-} effect is observed apparently on the line number 2 (see Fig. 3(b)) when dipolar contrast is changed into contrast corresponding to VS^{-}.

The modeling results show that the chirality direction in the US $\Rightarrow$ VS process is determined by the position of probe relative to particle. According to the situation presented in Fig. 5, if the probe is moved along the top edge of particle, a vortex with the counterclockwise orientation is nucleated. In the opposite case, when the probe is moved along the bottom region of particle, vortex nucleation with the clockwise orientation is observed.

It seams, that for elliptical particles with small lateral sizes one stage process of chirality changing is possible. The vortex annihilation and subsequent nucleation can be realized by single asymmetric passing over particle. In this case the MFM probe with high magnetic moment, that extremely perturbs particle magnetization, should be used. The same one stage process should be observed if the MFM tip traverses the elliptical particle in parallel with short axis. The asymmetry in particle shape and in probe passing is very important. For instance, one-pass MFM tip induced chirality changing in circle particles is impossible since any position of probe around particle is symmetric and vortex nucleation with right or left orientation will be realized in a random way.

4. Hedgehog-like states in ferromagnetic nanodisks

Here we will consider strong disturbance of the vortex magnetization in the circle nanodisk by the MFM probe field placed symmetrically above the particle (Fig. 6) [24].

First the numerical calculations for interaction between probe and vortex magnetization were performed on the base of LLG equations. The magnetization distributions for different parameters of probe magnetic moment are represented in Fig. 7. In case of low probe moment the spiral distribution of magnetization is formed (Fig. 7(b)), which caused by the influence of radial component of the probe field. With increasing of the probe field $\vec{H}_p$ the spiral distribution is straightened. For the fields $\vec{H}_p > \vec{H}_c$ (where $\vec{H}_c$ is some critical field) magnetization is drawn up along the radial component of the probe field and radial magnetization distribution (hedgehog state) is formed (Fig. 7(c)). The processes of radial distribution formation are accompanied by increasing of the core radius in case of $\vec{m}_p \uparrow\uparrow \vec{M}_c$ and by decreasing of the core radius in $\vec{m}_p \uparrow\downarrow \vec{M}_c$ case (where $\vec{M}_c$ is the core magnetization).

To find the critical parameters for the transition from spiral distribution of magnetization to radial one we considered theoretically the vortex magnetization disturbance in the circle

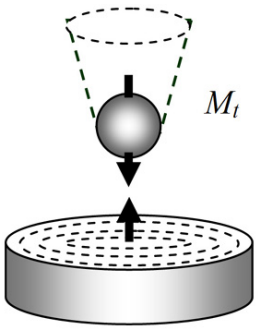

Figure 6. The schematic image of the MFM probe position above the disk.

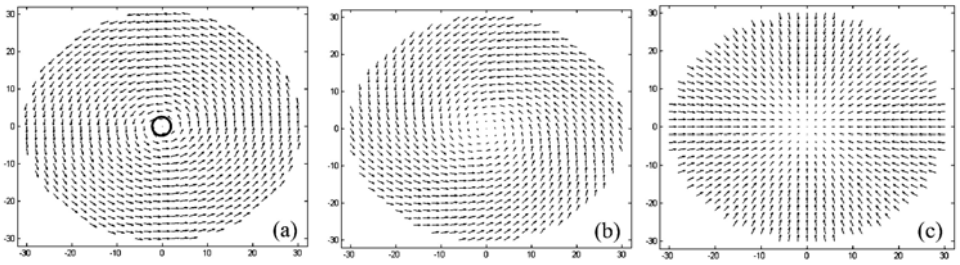

Figure 7. The disturbance of the vortex magnetization under influence of MFM probe field. (a) is undisturbed distribution. (b) is the disturbed distribution in the weak probe field. (c) is the radial distribution in the strong probe field. The probe position above the particle is indicated by circle.

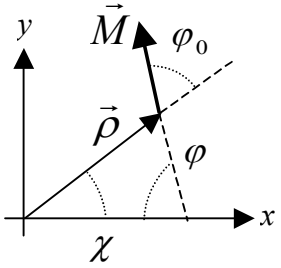

Figure 8. Schematic image to the magnetization disturbance simulation.

disk under magnetic field of the MFM probe placed over the center of the particle (Fig. 6). We analyzed the simple model of the spiral distribution which was described by constant angle φ_0 (Fig. 8). This simple model describe quite well the distribution in two extreme cases for vortex distribution ($\varphi_0 = \pm\pi/2$ realizing without probe field) and for radial distribution ($\varphi_0 = 0, \pi$ realizing in the strong probe field) as well. The direction of the magnetization vectors in this simple model is characterized by angle $\varphi = \chi + \varphi_0$.

The energy functional taking into account exchange energy W_{ex}, magnetostatic energy W_m and Zeeman energy can be written as

$$W = W_{ex} + W_m - \int \vec{H}\vec{M}dV \tag{5}$$

and after some simplification can be represented in the following form

$$W = W_0 + A\cos\varphi_0 + B\cos^2\varphi_0 . \tag{6}$$

In fact, coefficients A and B are determined by Zeeman and magnetostatic energies of the particle respectively. Minimizing the energy functional (6) we obtain following conditions for the angle φ_0

$$\begin{cases} \cos\varphi_0 = -A/2B, \text{ if } |A/2B| < 1, \\ \varphi_0 = 0, \pi, \text{ if } |A/2B| \geq 1. \end{cases} \tag{7}$$

It is easy to see that in case the absence of the probe field ($A = 0$) the vortex distribution is realized in the particle. For the strong probe fields when $|A/2B| < 1$ the spiral distribution is stable. And at last there are some critical parameters (value of magnetic moment in combination with height of probe position above the particle) when the transition from spiral to the radial distribution should be observed.

The analytical dependence for the $\cos\varphi_0$ value as the function of the probe radius was calculated on the base of the system (7) for the Co disks of 60 nm diameter and 20 nm height (Fig. 9). In calculations the probe height was chosen 100 nm but the probe radius was varied. The similar dependence for averaged value of $\cos\varphi_0$ at the same parameters was also calculated (Fig. 9) on the base of magnetization distributions which were generated in the LLG computer modeling. The calculated curves (Fig. 9) demonstrate good coincidence and the close critical parameters of the probe radius.

On the other hand, in the case of $\vec{m}_p \uparrow\downarrow \vec{M}_c$, when the *z* component of the probe field exceeds some coercive field $H_z > H_c$, the core of the vortex can change its magnetization direction. For a probe having the shape of a uniformly magnetized sphere with the radius *R* and with the residual magnetization of the material M_s, the *z* field component is equal to

$$H_z = \frac{8\pi M_s}{3}\left(\frac{R}{z}\right)^3 . \tag{8}$$

Estimations show that the field near the Co probe tip is of the order of 11 kOe. The results of a simulation of the magnetization reversal process of the core of the vortex in the MFM nonuniform probe field are presented in Fig. 10.

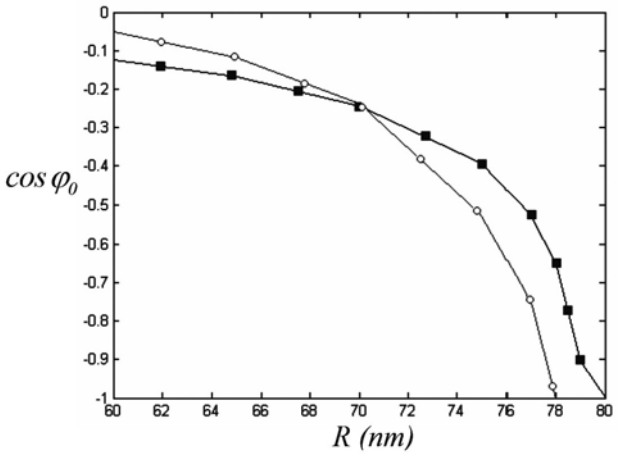

Figure 9. The dependence of $cos\varphi_0$ on the spherical probe radius R. The analytical results are indicated as the circles. The results of numerical calculations are indicated by squares.

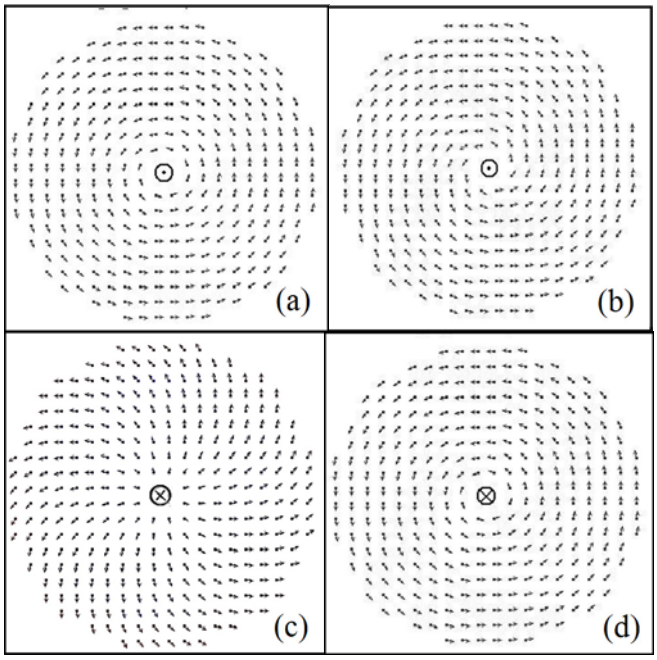

Figure 10. The magnetization reversal of a vortex core in the MFM probe field (case of $\vec{m}_p \uparrow\downarrow \vec{M}_c$). (a) is the initial vortex state with up-oriented core when probe is highly above the disk. (b) is the spiral state of vortex shell under radial component of probe field when the probe near the disc. (c) is changing of core orientation under Z component of probe field when probe close the disk. (d) is the final vortex state with other core orientation (probe highly above the disk).

The simulation was performed for a Co particle with diameter R = 200 nm and height h = 20 nm. In the initial state, the probe was exactly above the center of the particle (Fig. 10(a)) and then went down to the point of contact with the particle surface. The magnetization vectors in the particle tend to line up along the field lines under the action of the radial component of the probe field, since this leads to decreasing in the Zeeman energy. As a result, the magnetic vortex shell transforms from the vortex state (Fig. 10(a)) to the spiral state (Fig. 10(b)). As the probe and the particle approach each other, the magnetization direction of the core is reversed (Fig. 10(c)). When the probe moves away, the particle comes back into the vortex state with the opposite magnetization direction of the core of the vortex (Fig. 10(d)).

It should be noted that the magnetization reversal of the core of the VS of ferromagnetic nanoparticles in an external uniform field was previously studied in [25]. However, the external uniform field simultaneously affects all particles. The method of the magnetization reversal of the core by the MFM probe allows to control independently the magnetization state in each particle of an array. In the case of an inaccurate probe setting above the center of a particle, the magnetization reversal of the core by the MFM probe is complicated by the repulsion of the vortex to the periphery of the particle [23]. However, as the simulation showed, the vortex position near the center of a particle is rather stable, since the vortex displacement is accompanied by an increase in the magnetostatic energy. The permissible deviation of the probe from the center for magnetization reversal is up to 10% of the particle radius, which is reasonable from the viewpoint of the experimental observation of this phenomenon.

5. Core-shell interaction in magnetic vortex

As it was mentioned above, in the exchange approximation, a magnetic vortex is fourfold degenerate; i.e., all possible configurations with different vorticity signs (φ_0) and different directions of the vortex core (θ_0) have the same energies. However, it has been shown by Dzyaloshinski [26] and Moriya [27] that, in some low-symmetry crystals, the chiral symmetry can be broken due to spin–orbit interaction. From phenomenological point of view, this interaction is taken into account by adding Lifshitz invariants to an expansion of the free energy of the magnet; these invariants are of the form $J(\vec{M}\, rot\vec{M})$ [28], where J is the interaction constant. In bulk crystals whose lattice has an inversion center, this interaction is forbidden. However, in finite-size samples (nanostructures), this restriction can be removed [29] and, if the Dzyaloshinski interaction exists in a system, it can be detected. The existence of vortex magnetic states of ferromagnetic nanoparticles makes it possible to use them as an object for studying the chiral-symmetry effects in nanosystems. If there is no correlation between the sign of the vorticity and the magnetization direction in the vortex core, the chiral magnetic symmetry is conserved in such particles; in the opposite case, this symmetry is violated. We studied experimentally such effects in ferromagnetic nanodisks where the magnetization distribution has the form of a single conical vortex [30].

The magnetization direction in a vortex core can be controlled by preliminary magnetization (to saturation) of the disk in an external magnetic field applied perpendicular to the disk plane. Therefore, the experimental problem is reduced to finding the sign of the

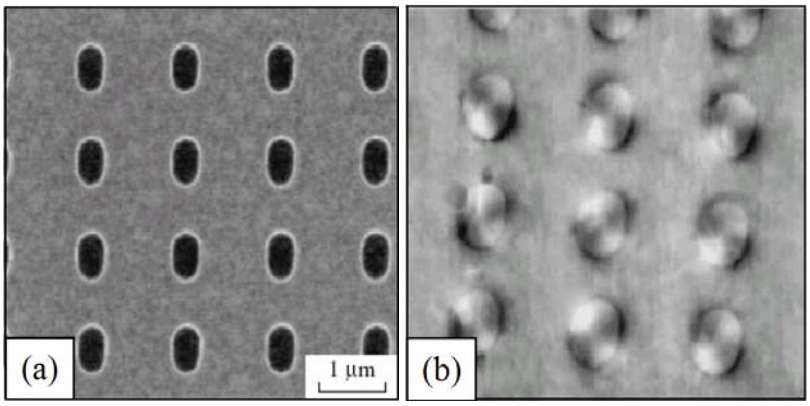

Figure 11. Experimental images of a fragment of a lattice of Co disks: (a) is SEM microphotograph obtained in the secondary-electron mode. (b) is the MFM image.

vorticity and determining the number of left- and right-handed vortexes that appear when the external magnetic field is switched off. In our experiments, we studied square lattices of 750 x 450 nm cobalt disks with 25-nm thickness (Fig. 11(a)) having a close-to-elliptic shape. The lattice period was approximately 1.5 μm.

To visualize the magnetization distributions in particles, we used magnetic force microscopy. As mentioned above, the vorticity sign in elliptical nanodisks can be uniquely determined from the configuration of white and black segments in the MFM image of the vortex [10, 17, 18, 31] (Fig. 11(b), compare with Fig. 2).

Before the main experiments, the systems of ferromagnetic disks were subjected to additional checks and selection. Several identical particle lattices have been fabricated containing 256 (16×16) pieces each. Disks with visible geometrical defects or asymmetric shapes, which was monitored using scanning electron microscopy and atomic force microscopy (AFM), were rejected. Systems of magnetic particles containing many imperfect disks were not used in the main experiment. For the lattices that passed this first selection stage, the coordinates of the rejected particles were fixed. For additional verification of the quality and shape of the selected particles, MFM studies of the residual nanodisk states were performed after magnetizing the disks along various directions in the disk plane. The direction of the magnetization field was chosen parallel to the long axis of a particle in the first series of preliminary experiments and parallel to the short axis in the second series. After magnetizing nanoparticles to saturation along their long axes and decreasing the external field to zero, the numbers of formed left- and right-handed vortices were approximately equal. The same results were also obtained when studying the residual states after magnetizing disks along the short axis. It should be noted that reversing the direction of the applied field did not affect the obtained result. Therefore, possible defects in the particle shape that we were unable to visualize are not important and do not affect the residual states of nanoparticles magnetized along the normal to the disk plane in the main experiment. Using all these procedures, we selected an area of one of the lattices containing 100 identical particles for the basic measurements. During the measurements, the preliminary magnetization in the direction

perpendicular to the sample plane was produced by applying an external magnetic field of 20 kOe, which exceeds the saturation field (~12 kOe) of the cobalt film used to form the ferromagnetic particles. The deviation of the external field from the normal to the sample surface did not exceed 5°.

The experimental MFM image shown in Fig. 11(b) is obtained for a typical residual state of a small fragment of a nanoparticle array. In comparing it with simulated images (Fig. 2), we see well that the magnetization distribution in each particle is one-vortical. We performed two series of experiments distinguished by the direction of the magnetizing field: in the first series, the field was directed upwards (↑) from the substrate, and, in the second series, downwards (↓) to the substrate. To increase the size of the sampling, several magnetization procedures were performed for each series and the statistics of vortical states were calculated. Above all, it appeared that approximately half of the particles change the vorticity sign for a single magnetization procedure. It should also be noted that no correlations between the states of neighboring particles were observed, which indicates the absence (or weakness) of interaction between the neighboring ferromagnetic disks. This fact allowed us to assume that the magnetizations of different particles are reversed independently of one another. Therefore, we can process the entire particle array statistically without performing experiments on a separate area of a particle array. Thus, we can make conclusions about the probability of the appearance of the left- and right-handed vortical distributions for a fixed direction of the vortex core polarization. Statistical processing of the obtained MFM images performed under the assumption of a bimodality of distributions [32] gives the following values of the probability of realizing right-handed vortices for different directions of the magnetizing field: $p\uparrow = 0.49 \pm 0.02$ and $p\downarrow = 0.51 \pm 0.03$. Accordingly, for the left-handed vortices, we have $p\uparrow = 0.51 \pm 0.02$ and $p\downarrow = 0.49 \pm 0.03$. The large error in the case $p\downarrow$ is caused by a smaller sampling.

Thus, our first experiments indicate the equivalence of left- and right-handed vortices in ferromagnetic cobalt particles of the size and shape under study. It should be noted also that the method used in this study is based on finding the populations of nanoparticle states with different vorticity signs. We assumed that, if the energies of these states were different, their populations would be different after the decay of an unstable state with a perpendicular magnetization. Since the preliminary magnetization was performed at room temperature, it is probable that, due to thermal fluctuations (which are especially strong in high magnetic fields), transitions between states with opposite vorticity signs are possible. Therefore, the final solution to the problem of the equivalence of left- and right handed vortices in ferromagnetic nanoparticles must be provided by low-temperature experiments on their magnetization.

6. Conclusion

Thus, in this paper we considered possible ways for control of vortex state parameters φ_0 and θ_0 using non-homogeneous field induced by tip of magnetic force microscope. First, we demonstrated transitions between vortex states with different chirality $\varphi_0 = \pm \pi / 2$ by means of two stage processes $\mathrm{VS}^{+(-)} \Rightarrow \mathrm{US} \Rightarrow \mathrm{VS}^{-(+)}$ under the action of non-homogeneous magnetic field of the MFM probe. It was shown that the necessary condition for these transitions is the asymmetry of the lateral components of

the MFM probe field. Second, we predicted the critical behaviour during transition between vortex ($\varphi_0 = \pm \pi/2$) and hedgehog ($\varphi_0 = 0, \pi$) states in sufficiently strong magnetic field with radial symmetry. Third, we investigated experimentally possibility for coupling between phase shift φ_0 and core polarization θ_0 for vortex state, which is possible due to spin -orbital interaction. Altogether the control and creation of discussed distributions of magnetization in ferromagnetic nanoparticles may be interesting for investigation of novel transport phenomena in non-homogeneous magnetic conductors [33, 34].

Acknowledgements

The authors are very thankful to B.A.Gribkov, S.A.Gusev, S.N.Vdovichev, A.Yu. Klimov, V.V.Rogov, D.S.Nikitushkin, O.L.Yermolaeva, I.M.Nefedov, I.R.Karetnikova and I.A.Shereshevsky for fruitful cooperation.

This work was partly supported by Russian foundation for basic researches and by EC through the NANOSPIN project (contract NMP4-CT-2004-013545).

References

1. M.Natali, Y.Chen, Magnetization reversal and vortex chirality correlation in ferromagnetic dot arrays, paper in this book.
2. A.A.Fraerman, S.A. Gusev, I.R.Karetnikova, L.A.Mazo, I.M.Nefedov, Yu.N.Nozdrin, M.V.Sapozhnikov, I.A.Shereshevsky, L.A.Suhodoev, Phys. Rev. B, **65**, 64424 (2002).
3. A.A.Fraerman, I.R.Karetnikova, I.M.Nefedov, I.A.Shereshevskii, M.A.Silaev, Phys. Rev. B, **71**, 094416, (2005).
4. D.Rugar, H.J.Mamin, P.Guethner, S.E.Lambert, J.E.Stern, I.McFadyen, T.Yogi, J. Appl. Phys., **68**, 1169-1183 (1990).
5. A.M.Kosevich, V.A.Voronov, I.V.Manzhos, Sov. Phys. JETP, **57**, 86 (1983).
6. R.P.Cowburn, D.K.Koltsov, A.O.Adeyeye, M.E.Welland, D.M.Ticcker, Phys. Rev. Lett., **83**, 1042 (1999).
7. V.Novosad, M.Grimsditch, J.Darrouzet, J.Pearson, S.D.Bader, V.Metlushko, K.Guslienko, Y.Otani, H.Shima, K.Fukamichi, Appl. Phys. Lett., **82**, 3716. (2003).
8. H.P.Oepen, H.Hopster, SEMPA studies of thin film structures and exchange coupled layers, p.137-167 in the book "Magnetic Microscopy of Nanostructures" eds H.Hopster, H.P.Oepen, Springer, 2003.
9. M.Grimsditch, P.Vavassori, V.Novosad et al, Phys. Rev. B, 65, 172419 (2002)
10. A.Fernandez, C.J.Cerjan, J. Appl. Phys., **87**, 1395 (2000).
11. M.Schneider, H.Hoffmann, J.Zweck, Appl. Phys. Lett., **79**, 3113 (2001).
12. E.D.Boerner and H.N.Bertran, IEEE Trans. Magn., **33**, 3152 (1997).
13. M.Kleiber, F.Kümmerlen, M.Löhndorf, A.Wadas, D.Weiss, R.Wiesendanger, Phys. Rev. B, **58**, 5563 (2002).
14. X.Zhu, P.Grütter, V.Metlushko, B.Ilic, Phys. Rev. B, **66**, 024423 (2002).
15. X.Zhu, P.Grütter, V.Metlushko, B.Ilic, J. Appl. Phys., **91**, 7340 (2002).
16. A.A.Fraerman, B.A.Gribkov, S.A.Gusev, V.L.Mironov, N.I.Polushkin, S.N.Vdovichev, Physics of Low – Dimensional Structures, no1/2, 117, (2004).
17. J.Chang, V.L.Mironov, B.A.Gribkov, A.A.Fraerman, S.A.Gusev, S.N.Vdovichev, J. Appl. Phys., **100**, 104304-1-7 (2006).
18. V.L.Mironov, B.A.Gribkov, A.A.Fraerman, S.A.Gusev, S.N.Vdovichev, I.R.Karetnikova, I.M.Nefedov, I.A.Shereshevsky, J. Magn. Magn. Mater., **312**, 153-157 (2007).
19. I.L.Prejbeanu, N.Natali, L.D.Buda, U.Ebels, A.Lebib, Y.Chen, K.Ounadjela, J. Appl. Phys. **91**, 7343 (2002).

20. http://math.nist.gov/oommf
21. A.A.Fraerman, L.Belova, B.A.Gribkov, S.A.Gusev, A.Yu.Klimov, V.L.Mironov, D.S. Nikitushkin, G.L.Pakhomov, K.V.Rao, V.B.Shevtsov, M.A.Silaev, S.N.Vdovichev, Phys. Low – Dim. Struct., 1/2, 35 (2004).
22. A.Fernandez, M.R.Gibbons, M.R.Wall, C.J.Cerjan, J. Magn. Magn. Mater. **190**, 71 (1998).
23. V.L.Mironov, O.L.Yermolaeva, J. Surf. Invest., issue **1**, no. 4, 466 (2007).
24. V.V.Chernov, O.L.Yermolaeva, A.A.Fraerman V.L.Mironov, Proceedings of XI International symposium "Nanophysics and nanoelectronics 2007" (N.Novgorod, March 10-14, 2007) p. 494-495.
25. T.Okuno, K.Shigeto, T.Ono, K.Mibu, T.Shino, J. Magn. Magn. Mater., **240**, 1 (2002).
26. I.E.Dzyaloshinski, Zh. Éksp. Teor. Fiz., **32**, 1547 (1957) [Sov. Phys. JETP **5** , 1259 (1957)].
27. T.Moriya, Phys. Rev. Lett., **4**, 228 (1960).
28. L.D.Landau, E.M.Lifshitz, Course of Theoretical Physics, Vol. 8: "Electrodynamics of Continuous Media" (Nauka, Moscow, 1982; Pergamon, Oxford, 1984).
29. A.N.Bogdanov, U.K.Robler, Phys. Rev. Lett., **87**, 037203 (2001).
30. S.N.Vdovichev, B.A.Gribkov, S.A.Gusev, V.L.Mironov, D.S.Nikitushkin, A.A.Fraerman, V.B.Shevtsov, Physics of the Solid State, **48**(10), 1902 (2006).
31. M.Grimsditch, P.Vavassori, V.Novosad, V.Metlushko, H.Shima, Y.Otani, K.Fukamichi, Phys. Rev. B, **65**, 172419 (2002).
32. D.J.Hudson, "Statistics: Lectures on Elementary Statistics and Probability" (CERN, Geneva, 1964; Mir, Moscow, 1967).
33. J.Fabian, S.Das Sarma, Phys. Rev. B, **66**, 024436 (2002).
34. F.Zhou, Phys. Rev. B, **70**, 125321 (2004).